The Journal of Headache and Pain

RESEARCH

Open Access

Genetic influence of the brain imaging phenotypes, brain and cerebrospinal fluid metabolites and brain genes on migraine subtypes: a Mendelian randomization and multi-omics study

Ping-An Zhang[1†], Jie-Lin Wang[2†], Mei-Hua Dong[1†], Xiang-Chun Huang[2], Nai-Jian Li[1*], Run-Dong Qin[1*] and Jing Li[1*]

Abstract

Background Migraine is a complex neurological disorder with high prevalence but unclear pathogenesis. Numerous studies have suggested that migraine is associated with alterations in brain imaging phenotypes (BIPs) and dysregulation of cerebrospinal fluid (CSF) and brain metabolism; however, causal evidence remains limited. Mendelian randomization (MR) offers a powerful approach for inferring causality using genetic instruments.

Methods Firstly, we conducted linkage disequilibrium score regression (LDSC) to evaluate genetic correlations between migraine, including the migraine with aura (MA) and migraine without aura (MO) subtypes, and BIPs, CSF, and brain metabolites. Traits that showed genetic correlations with migraine, MA, or MO were retained for subsequent MR analysis with the corresponding migraine phenotype. Traits showing significant correlations were analyzed using bidirectional two-sample MR (TSMR), followed by two-step TSMR to identify cross-omics mediation effects. Additionally, We also applied summary-data-based MR (SMR) to detect brain-region-specific genes with potential causal effects. Enrichment analyses (KEGG, GO, PPI, transcription factor, and miRNA networks) were conducted to further explore underlying mechanisms.

Results LDSC identified significant genetic correlations with 73 BIPs and 40 metabolites for overall migraine, 71 BIPs and 37 metabolites for MA, and 49 BIPs and 62 metabolites for MO. Enrichment analysis revealed that genetically associated metabolites were predominantly involved in amino acid metabolic pathways. TSMR identified 6 BIPs and

†Ping-An Zhang, Jie-Lin Wang and Mei-Hua Dong contributed equally to this work.

*Correspondence:
Nai-Jian Li
naijian@126.com
Run-Dong Qin
407276157@qq.com
Jing Li
jingli1016@vip.163.com

Full list of author information is available at the end of the article

2 metabolites causally linked to overall migraine, 3 BIPs and 3 metabolites to MA, and 2 BIPs and 5 metabolites to MO. Most migraine-related BIPs mapped to the parietal lobe. Reverse MR analysis showed that overall migraine causally influenced 4 BIPs and 3 metabolites, while MA and MO affected 1 BIP and 1 metabolite, and 3 BIPs and 1 metabolite, respectively. Mediation analysis revealed five significant mediation pathways were identified. SMR analysis identified FAM83B and CIB2 consistently showing inhibitory effects across most regions. Enrichment analysis showed that these genes were predominantly involved in immune activation and cell adhesion.

Conclusions Our study integrates cross-omics analyses to investigate the causal links between brain structure, metabolic alterations, gene expression, and migraine including its MA and MO subtypes. These findings provide novel insights into the pathophysiological mechanisms and potential targets for intervention across migraine subtypes.

Graphical Abstract

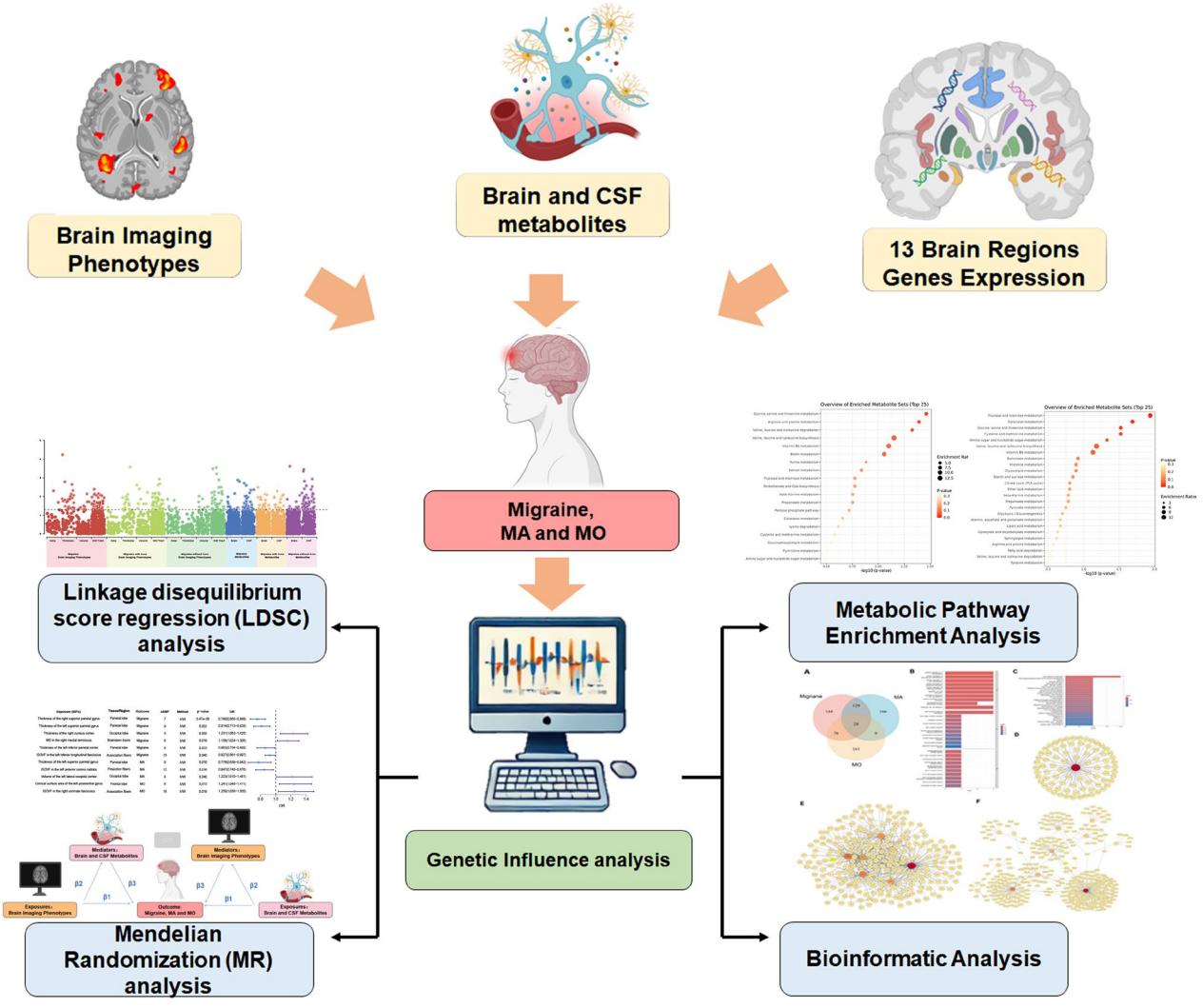

Keywords Migraine, Brain imaging phenotypes, Brain and cerebrospinal fluid metabolites, Mendelian randomization, Genome-wide association, Multi-omics

Introduction

Migraine, which includes two main subtypes—migraine with aura (MA) and migraine without aura (MO) [1]—affects approximately 14–15% of the global population [2]. It is characterized by recurrent headache episodes, often accompanied by nausea, photophobia, and phonophobia [3]. Despite its prevalence, the pathophysiological mechanisms of migraine remain inadequately understood. Given the significant global prevalence of migraine, its considerable health burden, and its

extensive impact on individuals and society, clarifying its pathophysiological mechanisms is crucial for alleviating the population's health burden and enhancing individual well-being.

Although the causes of migraine attacks remain unclear, numerous studies have suggested that migraines are significantly linked to brain structure and function, including brain metabolism and neuroimaging studies [4, 5]. For example, the application of phosphorus nuclear magnetic resonance (31P-NMR) spectroscopy revealed abnormal energy metabolism in the brains of migraine patients [6]. Dysfunction of glutamate and GABA metabolism can trigger migraines by disrupting the brain's balance between excitation and inhibition, leading to an imbalance in these key neurometabolites [7–9]. In addition, migraine has a higher prevalence in mitochondrial disorders [10]. Mitochondrial dysfunction plays a crucial role in the pathogenesis of migraines by disrupting energy metabolism, leading to excessive Ca2 + influx, increased free radical production, decreased mitochondrial membrane potential, and impaired oxidative phosphorylation [11]. This mitochondrial damage promotes neuronal apoptosis, lowers the pain threshold, and triggers migraine attacks. In addition to metabolic changes, structural abnormalities in the brain have also been documented. Studies have shown that individuals with migraines exhibit a high frequency of white matter abnormalities, silent infarct-like lesions, and volumetric changes in gray and white matter compared to controls [4]. These modifications occur during migraine ictal and interictal periods, reshaping cerebral, cerebellar, and brainstem structures while disrupting neuronal network integrity and functional dynamics [12, 13]..

Building upon the previous discussion of metabolic and structural alterations in migraine, it's important to note that changes in metabolite levels within the brain and CSF can significantly influence brain structure through mechanisms such as synaptic plasticity and neural remodeling. For example, in the chronic state of migraine, the brain or certain key areas of the brain may be in a constant state of low energy, leading to hyperactivation and sensitisation of the trigeminal vascular system [5]. Dysregulation of mitochondrial metabolites can lead to impaired energy homeostasis, oxidative stress, and neuronal apoptosis, further contributing to structural and functional abnormalities in the brain [14]. Conversely, structural changes in the brain may also affect metabolic pathways.Gray matter exhibits high metabolic activity, with approximately 70% of its energy expenditure dedicated to signaling processes such as synaptic transmission and action potentials. In contrast, white matter primarily consumes energy for nonsignaling functions, with only about 18% devoted to signaling, and its metabolism adjusts modestly in response to changes in cortical activity [15]. Moreover, region-specific gene expression patterns in the brain can modulate local metabolic activities and structural remodeling by regulating mitochondrial function, neurotransmitter synthesis, and neuroinflammatory responses. Given these complex interactions between gene expression, metabolic processes, and brain structure, studying these aspects separately would likely overlook critical cross-talk and potentially miss important mechanistic insights. Therefore, a multi-omics integrative approach is crucial for unraveling the pathophysiological mechanisms underlying migraine.

These observational studies are designed as case-control studies, making it difficult to determine the temporal sequence between exposure factors and disease outcomes or establish causal relationships. Mendelian randomization (MR) is a statistical method that uses genetic variations as instrumental variables and has been extensively utilized in evaluating causal relationships between exposures and outcomes in recent years [16]. This method effectively investigates risk factors that causally influence disease incidence [17, 18]. It is a reliable approach as it reduces the confounding factors that could distort the results and eliminates the possibility of the results being influenced by reverse causation bias [19, 20].

Previous studies have recognized the importance of identifying causal links between metabolites, brain imaging phenotypes (BIPs), and migraine. For instance, Hamzeh et al. explored the causal relationships between plasma metabolites and migraine [21]. However, they overlooked the fact that, given the tightly regulated molecular exchange imposed by the blood-brain barrier, peripheral metabolic changes may not fully reflect metabolic dysregulations within the central nervous system. Therefore, our study places particular emphasis on investigating causal relationships between brain and cerebrospinal fluid (CSF) metabolites and migraine. Similarly, Sun et al. and Mitchell et al. investigated causal associations between brain imaging-derived phenotypes and migraine [22, 23]. Compared to their research, building upon reliable segmentation methods and meaningful measurement approaches, we carefully selected 587 structural BIPs from the GWAS summary statistics provided by Smith et al. to avoid redundant phenotypes. Moreover, our study advances further by exploring the mediating effects of BIPs and metabolites, representing a comprehensive multi-omics approach. Additionally, we applied summary-data-based Mendelian randomization (SMR) analysis using cis-eQTL data across 13 brain regions to systematically assess brain region-specific gene expression causally associated with migraine and its subtypes for the first time. Integrating macro-level (BIPs), micro-level (metabolites), and molecular-level (gene expression) data, this multi-layered analytical framework

constitutes one of the most comprehensive genetic and functional studies of migraine to date. Our findings provide a foundation for future research and potential therapeutic strategies targeting metabolic and immune pathways.

Methods

Study design

Firstly, Linkage Disequilibrium Score Regression (LDSC) was used to explore the genetic correlations between BIPs, CSF and brain metabolite, and migraine, including its MA and MO subtypes. Traits that showed genetic correlations (rg-p-value < 0.05) with overall migraine, MA, or MO were retained for subsequent MR analysis with the corresponding migraine phenotype.

Secondly, to investigate potential mediation mechanisms and integrate metabolic and imaging omics layers, we conducted a two-step two-sample Mendelian randomization. In first step, a two-sample MR analysis was conducted to investigate the causal impact of BIPs and CSF and brain metabolite on migraine and its subtypes. In the second step, we conducted two additional two-sample MR analyses to further investigate the causal interrelationships of those BIPs and metabolites that showed significant associations (IVW $p < 0.05$) in the initial analysis. Specifically, we evaluated whether certain metabolites mediate the effect of BIPs on migraine, or whether BIPs mediate the effect of metabolites on migraine and calculated the mediation effect. Additionally, we conducted reverse MR to explore the causal effects of migraine and its subtypes on BIPs and on brain and CSF metabolites.

Thirdly, We used SMR analysis to access the causal effect of gene expression in different brain regions on migraine and its subtypes using 13 GWAS summary datasets documenting gene expression in these regions. Afterward, we performed bioinformatics investigations on these genes, encompassing Kyoto Encyclopaedia of Genes and Genomes (KEGG) pathway analysis, protein-protein interaction (PPI) analysis, transcription factor interaction prediction analysis, and miRNA interaction prediction analysis. Additionally, we utilised the MetaboAnalyst 6.0 platform (http://dev.metaboanalyst.ca/) to investigate the metabolic pathways and do an enrichment analysis of the metabolites [24]. Our MR analysis relies on three key assumptions: (1) that instrumental variables (IVs) are strongly associated with exposure factors, (2) that IVs are independent of any confounding variables, and (3) that IVs affect outcomes exclusively through the exposure of interest. These assumptions strengthen the validity of causal inferences in MR studies [25]. We adhered to the recommended standards outlined in the Strengthening the Reporting of Observational Studies in Epidemiology-Mendelian Randomization (STROBE-MR) checklist for our study (Supplement STROBE-MR-checklist) [26]. Figure 1 presents a concise summary of the research design.

Data source

The GWAS summary data of brain structural features were obtained from the IEU open GWAS project (https://gwas.mrcieu.ac.uk/datasets/). Smith et al. conducted a genome-wide association study derived from 33,224 participants from the UK Biobank. These imaging-derived phenotypes originated from three types of measurements: structural MRI, diffusion MRI (dMRI), and functional magnetic resonance imaging (fMRI) summary metrics [27]. From the initial 3,913 structural MRI-derived phenotypes, 587 BIPs related to brain structural features were selected (Supplementary Table 1). These 587 BIPs were further categorized based on the type of measurement into the following categories: regional and tissue volume, cortical area, cortical thickness, and white matter (WM) tract. The analysis also included 13 regional categories: Association fibers, Brainstem tracts, Commissural fibers, Frontal lobe, Insula, Limbic system, Limbic system fibers, Occipital lobe, Parietal lobe, Projection fibers, Subcortical region, Temporal lobe, and Total brain [28].

The GWAS summary data for CSF and brain metabolites derives from the most recent study by Cruchaga et al. [29]. Cruchaga et al. performed an MGWAS utilising extensive datasets of CSF ($n = 2{,}602$) and brain tissue ($n = 1{,}016$), uncovering novel genetic correlations for 440 CSF metabolites and 962 brain metabolites (Supplementary Table 2).

To avoid overlapping samples, we conducted a comprehensive analysis of genome-wide association studies (GWAS) for three types of migraine using the Finngen database (https://www.finngen.fi/en) [30]: Overall migraine (26894 cases, 374605 controls), MA (11757 cases, 374605 controls), and MO (9690 cases, 139,622 controls). Each case was diagnosed using the International Classification of Diseases (ICD) criteria from the Finnish Hospital Discharge Register. ICD-10 code G43 was used for migraine patients.

Selection of instrumental variables

In our forward and reverse MR analyses as well as the mediation analysis analysis, IVs underwent a rigorous screening to ensure validity. According to one of the three key assumptions of MR analysis: IVs must be strongly associated with exposures, we prioritized using a genome-wide significance threshold of $p < 5 \times 10^{-8}$ to ensure that the selected SNPs were strongly associated with the exposures [31]. When the number of SNPs meeting this threshold was too small (no more than three) to allow for sensitivity analyses, we adopted

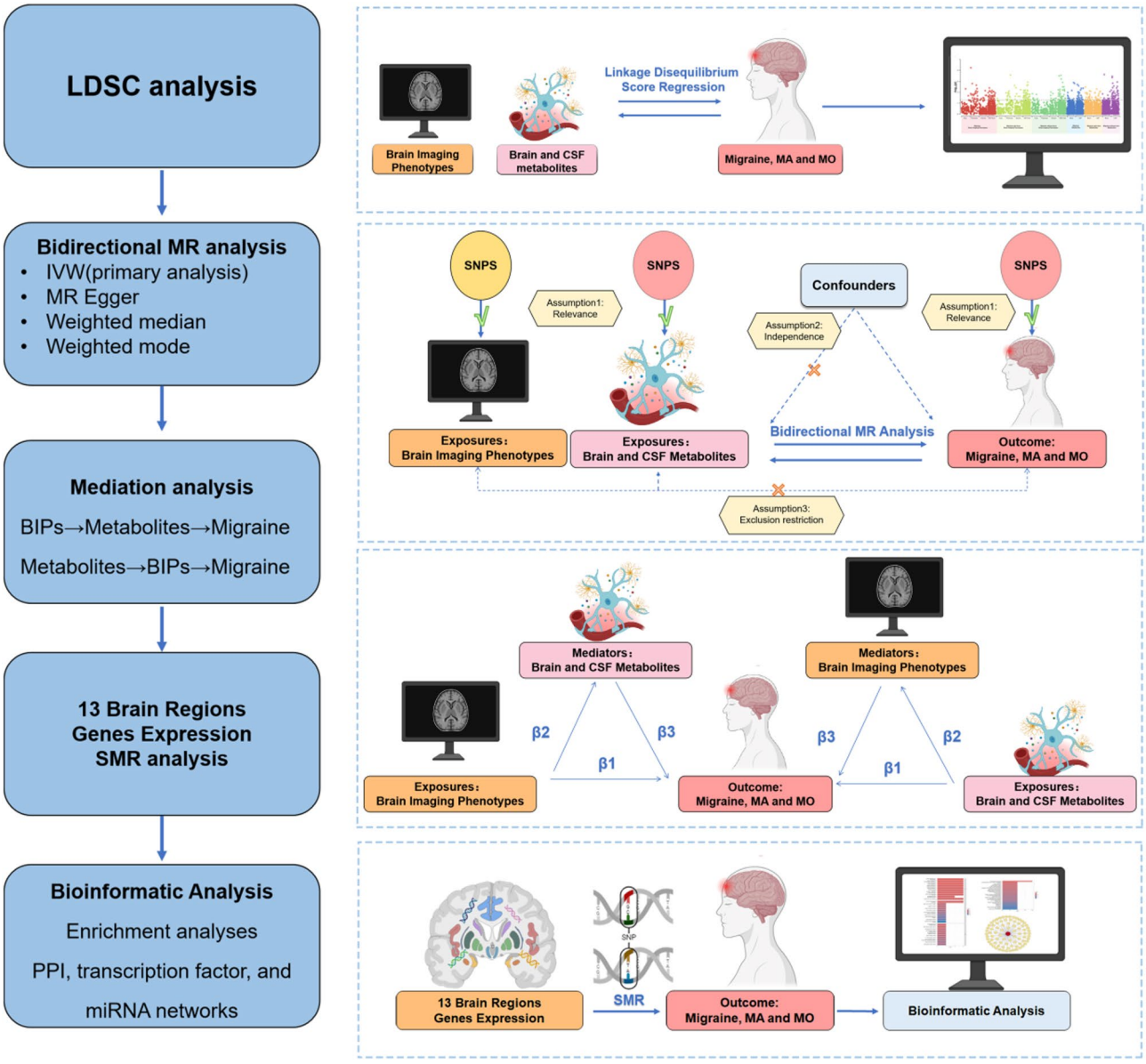

Fig. 1 Overall study design of the article

a relaxed threshold of $p < 5 \times 10^{-6}$ to obtain a sufficient number of SNPs [32]. These SNPs were then assessed for linkage disequilibrium using the "clump data" tool, with a threshold set to $r^2 < 0.01$ within a 10,000 kb window. This step ensured that the independent variables for each exposure were independent by excluding non-biallelic SNPs and those in linkage disequilibrium. To confirm that the remaining SNPs were strongly linked with the exposure, we excluded those with F-statistics below 10. SNPs with palindromic characteristics were systematically removed from the IVs. Finally, we ensured that the phenotype was relevant to the outcome by screening for confounding factors and removing such SNPs using the GWAS Catalog website (https://www.ebi.ac.uk/gwas).

Statistical analysis

Genetic correlation validation

Linkage Disequilibrium Score Regression (LDSC) is a widely used method for estimating genetic correlations between complex diseases and traits. In this study, we applied LDSC to estimate the genetic correlation between BIPs, CSF and brain metabolite, and migraine. The LD score of each SNP was calculated to infer its association strength with complex traits based on the concept of genetic linkage disequilibrium (LD) [33]. We excluded SNPs that did not match HapMap3 SNPs and those with a minor allele frequency below 0.01. Results are presented as the genetic correlation coefficient (rg) with standard error (SE). The rg ranges from −1 to 1,

with rg < 0 indicating a negative genetic correlation and rg > 0 indicating a positive genetic correlation. LDSC genetic correlation p-value (rg-p-value) below 0.05 were considered indicative of a possible genetic association. Results of LDSC analysis may not be available if one or both traits show insufficient heritability [34, 35].

Two-sample Mendelian randomization analysis

We performed a two-step TSMR analysis using several MR methods, including MR Egger, weighted median, inverse variance weighted (IVW), and weighted mode. We used the IVW method as the principal analysis, which is a robust MR method under the assumption of valid instrumental variables and balanced pleiotropy [36].

A causal association was considered statistically significant if the IVW p-value was below the Bonferroni-corrected threshold (i.e., 0.05 divided by the number of exposures tested at each stage of analysis), with no evidence of horizontal pleiotropy or heterogeneity. Associations with p-values less than 0.05 but exceeding the Bonferroni-corrected threshold, which also passed all sensitivity analyses, were interpreted as suggestive of potential causal effects [37, 38].

Sensitivity analysis

Heterogeneity was assessed using Cochran's Q test, where a p-value greater than 0.05 indicated the absence of heterogeneity [39]. To assess horizontal pleiotropy, we employed MR Eggar and MR-Presso analyses; a p-value greater than 0.05 suggested no evidence of horizontal pleiotropy. The MR-PRESSO method was used to detect and remove significant outliers, thus minimizing the impact of horizontal pleiotropy [31, 40]. Additionally, we carried out a leave-one-out study, systematically excluding each SNP to determine whether a single SNP disproportionately affected the results [41].

Reverse MR analysis

To further assess whether migraine and its subtypes exert a reverse causal effect on BIPs and on brain and CSF metabolites, we performed reverse MR analyses. In these analyses, migraine or its subtype served as the exposure, using its associated SNPs as instrumental variables, while BIPs and brain and CSF metabolites were treated as outcomes. The analytical process followed the same methodology as the forward MR analysis.

Mediation analysis

We applied a two-step, two-sample Mendelian randomization framework to examine whether brain imaging phenotypes mediate the causal link between metabolites and migraine, and whether metabolites mediate the effect of brain imaging phenotypes on migraine. First, in previous sections of the study, we identified BIPs and metabolites showing significant causal associations with overall migraine or its subtypes (MA, MO) without evidence of heterogeneity or horizontal pleiotropy. Second, based on those BIPs and metabolites with IVW p-values < 0.05 from the first-step analysis, we conducted additional two-sample MR analyses to investigate the potential causal relationships between BIPs and metabolites—specifically assessing whether BIPs influence metabolite levels or, conversely, whether metabolites affect BIPs. Third, we selected mediator candidates, whose effect is logically consistent with potential mediators based on the directions of the effect values: β_1 represents the effect of the exposure on the outcome, β_2 represents the effect of the exposure on the mediator, and β_3 represents the effect of the mediator on the outcome. When β_1 was positive, both β_2 and β_3 were required to be in the same direction (either both positive or both negative); when β_1 was negative, β_2 and β_3 were required to have opposite directions. The mediation effect was calculated using the coefficient product technique (mediation effect = $\beta 2 \times \beta 3$), and the proportion mediated was estimated as $(\beta_2 \times \beta_3) / \beta_1$ [42, 43].

SMR methods and bioinformatic analysis of gene expression across various brain regions

We utilized expression quantitative trait loci (eQTLs) from multiple brain regions as proxies for gene expression, with eQTL data from the GTEx Consortium (https://gtexportal.org/home/datasets). To evaluate the potential causal influence of these genes on migraine, we performed SMR analysis, applying eQTL selection criteria of a minor allele frequency (MAF) exceeding 1% and a significance threshold of $p < 5e\text{-}08$, restricting the study to cis-eQTLs. We selected genetic instrumental variables (IVs) to represent brain structure and gene expression in these locations. Furthermore, we found single nucleotide polymorphisms (SNPs) located within a 100 kb proximity of the target genes that were substantially associated with gene expression in multiple brain regions. The causal effect of gene expression on migraine risk was estimated by integrating the influence of eQTLs on gene expression (βSNP-eQTL) with their impact on migraine susceptibility (βSNP-migraine). Associations were considered significant when P-values were below 0.05, and HEIDI test results with P-values more significant than 0.05 supported the presence of a shared causal variant rather than linkage disequilibrium. Our findings suggest that gene expression at these loci may contribute causally to migraine risk, with several target genes commonly expressed across migraine and its subtypes, MA and MO. Further bioinformatics analyses were conducted on these genes, including KEGG pathway enrichment, PPI network construction, and transcription factor and miRNA interaction prediction analyses. We used the Network

Fig. 2 (See legend on next page.)

(See figure on previous page.)

Fig. 2 Genetic correlations between BIPs, CSF and brain metabolite, and migraine. (**A**) Manhattan plot of LDSC results for BIPs and CSF/brain metabolites across migraine phenotypes. (**B**)Venn diagram illustrating the genetic correlation of BIPs with Migraine, MA, and MO. Numbers represent unique and shared metabolites among the groups. (**C**).Venn diagram illustrating the genetic correlation of metabolites with Migraine, MA, and MO. Numbers represent unique and shared metabolites among the groups. (**D**) Stacked bar plot showing the classification of metabolites with significant genetic correlations to migraine phenotypes. (**E**–**G**) KEGG pathway enrichment analyses of migraine-related metabolites for overall migraine (**E**), MA (**F**), and MO (**G**)

Analyst website (https://www.networkanalyst.ca/) for these analyses [44].

Metabolic pathways and enrichment analysis

To recognize CSF and brain metabolites (rg-p-value < 0.05), we utilized MetaboAnalyst 6.0 (https://www.metaboanalyst.ca/) [24] to perform metabolic pathway analysis to ascertain probable metabolic pathways associated with the biological processes of migraine. This work utilized the KEGG database.

Result

Genetic correlations between BIPs, CSF and brain metabolite, and migraine

We used LDSC to investigate the genetic associations between BIPs, CSF and brain metabolites, and migraine (Fig. 2A). The LDSC analyses indicated that 73 BIPs had a statistically significant genetic connection with overall migraine, of which 18 were negatively genetically correlated, and 55 were positively genetically correlated. Simultaneously, the LDSC data indicated that 40 CSF and brain metabolites had statistically significant genetic correlations with migraine(16 negatively genetic correlations and 24 positively genetic correlations), with an rg-p-value of less than 0.05.

The genetic associations between the MA and MO subtypes with BIPs and metabolites were also analyzed using LDSC. 71 BIPs had a statistically significant genetic association with MA, of which 21 were negatively correlated, and 50 were positively correlated. 49 BIPs exhibited a statistically significant genetic association with MO, comprising 26 with a negative genetic correlation and 23 with a positive genetic correlation. Our research identified 7 BIPs that exhibit genetic associations with overall migraine, as well as MA and MO subtypes (Fig. 2B).

The LDSC analysis revealed that 37 CSF and brain metabolites exhibited statistically significant genetic correlations with MA, including 9 with negative correlations and 28 with positive correlations. Additionally, 62 CSF and brain metabolites were significantly correlated with MO, with 32 showing negative correlations and 30 showing positive correlations. Our findings identified seven metabolites that exhibit concurrent genetic correlations with overall migraine and the MA and MO subtypes (Fig. 2C). Detailed of the LDSC analysis result was show in Supplementary Tables 3–4.

Next, we assessed the biochemical classes of metabolites with significant genetic correlations to migraine and found that amino acids predominated in overall migraine, whereas lipids and xenobiotics were more prominent in both MA and MO (Fig. 2D).

Finally, KEGG pathway enrichment of these metabolites highlighted distinct metabolic signatures for each phenotype. For overall migraine (Fig. 2E), pathways such as glycine, serine, and threonine metabolism, arginine and proline metabolism, and valine, leucine, and isoleucine biosynthesis and degradation were enriched, suggesting that metabolites with genetic associations are significantly related to amino acid metabolism. In the case of MA, KEGG enrichment analysis revealed that fructose and mannose metabolism, along with galactose metabolism, were notably enriched, highlighting the importance of sugar and carbohydrate metabolism in the development of MA. Additionally, numerous amino acid-related pathways were also enriched. For MO (Fig. 2G), amino acid metabolism pathways were prominently enriched, further emphasizing the role of amino acids in this subtype. Across all migraine phenotypes amino acid metabolism emerged as a critical factor.

Exploring the causal effect of BIPs on migraine

The LDSC analysis revealed that 73 BIPs had a statistically significant genetic association with overall migraine, 71 BIPs with MA, and 49 BIPs with MO. These BIPs were subsequently analyzed in TSMR to investigate their causal effects on the corresponding migraine phenotypes.

Notably, each increase in thickness of the right superior parietal gyrus was associated with a lower migraine risk (OR 0.760, 95% CI 0.665–0.869; $p = 5.47 \times 10^{-5}$), a finding that remained significant after Bonferroni correction. Similarly, greater thickness of the left superior parietal gyrus also conferred protection (OR 0.814, 95% CI 0.713–0.928; $p = 0.002$). In contrast, increased thickness of the right cuneus cortex raised migraine risk (OR 1.231, 95% CI 1.063–1.425; $p = 0.005$), as did higher diffusion tensor mode (MÒ) in the right medial lemniscus (OR 1.156, 95% CI 1.024–1.305; $p = 0.019$). Thickness of the left inferior parietal cortex (OR 0.863, 95% CI 0.754–0.988; $p = 0.033$) and ISOVF in the left inferior longitudinal fasciculus (OR 0.927, 95% CI 0.861–0.997; $p = 0.040$) also showed protective effects.

For MA, two BIPs conferred protection. Higher Thickness of the left superior parietal gyrus was associated with a reduction in MA risk (OR 0.776, 95% CI 0.639–0.942; $p = 0.010$), and an increased ISOVF in the left anterior corona radiata reduced MA risk (OR 0.847, 95% CI

0.740–0.970; $p = 0.016$). While the Volume of the left lateral occipital cortex increased MA risk (OR 1.223, 95% CI 1.010–1.481; $p = 0.040$).

In MO, two BIPs increased susceptibility. Elevated greater Cortical surface area of the left postcentral gyrus increased risk (OR 1.241, 95% CI 1.048–1.471; $p = 0.013$), and higher ISOVF in the right uncinate fasciculus was associated with a increase in MO risk (OR 1.250, 95% CI 1.038–1.505; $p = 0.019$). The forest plot summarizing these results is shown in Fig. 3A. All BIPs with a causal effect on migraine and its MA and MO subtypes are summarized in Supplementary Tables 5–7.

Exploring the causal effect of CSF and brain metabolite on migraine

The LDSC analysis identified 40 CSF and brain metabolites genetically correlated with overall migraine, 37 with MA, and 62 with MO, which were subsequently analyzed using TSMR to investigate their causal effects on the corresponding migraine phenotypes.

Two metabolites demonstrated significant causal effects on overall migraine: pyridoxal (CSF) was associated with a reduced risk (OR 0.660, 95% CI 0.477–0.914; $p = 0.012$), and 3-ureidopropionate (CSF) also lowered the risk (OR 0.863, 95% CI 0.754–0.987; $p = 0.031$).

In MA, three metabolites increased risk: pyridoxal (CSF) (OR 1.231, 95% CI 1.063–1.425; $p = 0.005$), 3-hydroxyhexanoate (brain) (OR 1.203, 95% CI 1.010–1.433; $p = 0.038$), and glycosyl ceramide (d18:1/23:1, d17:1/24:1) (brain) (OR 1.101, 95% CI 1.005–1.207; $p = 0.038$).

For MO, two CSF metabolites were protective: 1-oleoyl-GPC (18:1) (OR 0.587, 95% CI 0.388–0.887; $p = 0.011$) and lysine (OR 0.356, 95% CI 0.157–0.808; $p = 0.014$). In contrast, three metabolites increased MO risk: N-acetylglycine (CSF) (OR 1.579, 95% CI 1.046–2.382; $p = 0.030$), X-15,674 (CSF) (OR 1.267, 95% CI 1.011–1.589; $p = 0.040$), and 2-piperidinone (CSF) (OR 1.123, 95% CI 1.005–1.255; $p = 0.041$). All the causal associations were summarized in the forest plot shown in Fig. 3B. All metabolites with a causal effect on migraine and its MA and MO subtypes are summarized in Supplementary Tables 8–10.

Reverse MR analysis of the causal effects of migraine on BIPs, CSF, and brain metabolites

We then conducted a reverse MR analysis to investigate the causal relationship of Migraine on BIPs, CSF, and Brain Metabolites. Results from the IVW reverse MR analyses indicated that migraine and its subtypes showed no significant causal associations with any of the BIPs or metabolites identified in the forward MR. However, exploratory reverse MR revealed that migraine and its subtypes exerted causal effects on eight additional BIPs and five metabolites.

Overall migraine was found to causally increase ISOVF in the right uncinate fasciculus (OR 1.141, 95% CI 1.047–1.242; $p = 0.003$) and to decrease MO in the right superior thalamic radiation(OR 0.907, 95% CI 0.833–0.987; $p = 0.024$), Cortical surface area of the left postcentral gyrus(OR 0.911, 95% CI 0.837–0.991; $p = 0.030$), and MD in the middle cerebellar peduncle (OR 0.916, 95% CI 0.841–0.998; $p = 0.045$). MA increased the level of Thickness of the left postcentral gyrus (OR 1.042, 95% CI 1.001–1.083; $p = 0.043$). MO decreased the level of Cortical surface area of the right rostral middle cingulate cortex (OR 0.952, 95% CI 0.921–0.983; $p = 0.003$) and Volume of the right rostral middle cingulate cortex (OR 0.958, 95% CI 0.927–0.990; $p = 0.010$) and increaded the level of ISOVF in the genu of corpus callosum (OR 1.035, 95% CI 1.001–1.069; $p = 0.042$).The reverse MR results showing the causal effects of migraine on Bips are illustrated in the forest plot in Fig. 3C.

Overall migraine was associated with increased levels of methylmalonate (OR 1.114, 95% CI 1.013–1.226; $p = 0.026$), ascorbic acid 3-sulfate (OR 1.123, 95% CI 1.013–1.244; $p = 0.027$), and alpha-hydroxyisovalerate (OR 1.141, 95% CI 1.002–1.299; $p = 0.046$). MA was linked to elevated levels of N-acetyltaurine (OR 1.042, 95% CI 1.004–1.082; $p = 0.031$), while MO increased the level of salicylate in CSF (OR 1.364, 95% CI 1.029–1.808; $p = 0.031$). The reverse MR results showing the causal effects of migraine on metabolites are illustrated in the forest plot in Fig. 3D. Further details of the reverse MR analysis can be found in Supplementary Tables 11–16.

Mediation analysis

Subsequently, we applied a two-step, two-sample Mendelian randomization framework to investigate whether brain imaging phenotypes mediate the causal relationship between metabolites and migraine, and conversely, whether metabolites mediate the effect of brain imaging phenotypes on migraine.BIPs and metabolites with IVW p-values < 0.05 from previous analyses were selected for TSMR analysis, and the detailed results are provided in Supplementary Table 7. We then screened for BIPs and metabolites that demonstrated both a causal relationship and logically consistent effect directions based on β values. Ultimately, five significant mediation pathways were identified, as summarized in Table 1; Fig. 4.

For overall migraine, the thickness of the right superior parietal gyrus was found to exert protective effect through the CSF metabolite nucleotide, with a mediated proportion of 5.33%. Similarly, the effect of nucleotide in CSF on overall migraine was partially mediated by the thickness of the left superior parietal gyrus, with a mediation proportion of 19.69%.

A

Exposure (BIPs)	Tissue/Region	Outcome	nSNP	Method	p−value	OR
Thickness of the right superior parietal gyrus	Parietal lobe	Migraine	7	IVW	5.47e−05	0.760(0.665−0.869)
Thickness of the left superior parietal gyrus	Parietal lobe	Migraine	9	IVW	0.002	0.814(0.713−0.928)
Thickness of the right cuneus cortex	Occipital lobe	Migraine	5	IVW	0.005	1.231(1.063−1.425)
MO in the right medial lemniscus	Brainstem tracts	Migraine	8	IVW	0.019	1.156(1.024−1.305)
Thickness of the left inferior parietal cortex	Parietal lobe	Migraine	8	IVW	0.033	0.863(0.754−0.988)
ISOVF in the left inferior longitudinal fasciculus	Association fibers	Migraine	15	IVW	0.040	0.927(0.861−0.997)
Thickness of the left superior parietal gyrus	Parietal lobe	MA	9	IVW	0.010	0.776(0.639−0.942)
ISOVF in the left anterior corona radiata	Projection fibers	MA	12	IVW	0.016	0.847(0.740−0.970)
Volume of the left lateral occipital cortex	Occipital lobe	MA	8	IVW	0.040	1.223(1.010−1.481)
Cortical surface area of the left postcentral gyrus	Frontal lobe	MO	6	IVW	0.013	1.241(1.048−1.471)
ISOVF in the right uncinate fasciculus	Association fibers	MO	16	IVW	0.019	1.250(1.038−1.505)

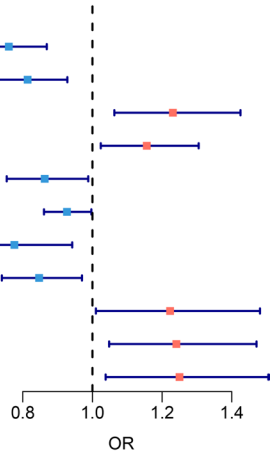

B

Exposure (Metabolites)	Outcome	nSNP	Method	p−value	OR
pyridoxal (CSF)	Migraine	15	IVW	0.012	0.660(0.477−0.914)
3−ureidopropionate (CSF)	Migraine	17	IVW	0.031	0.863(0.754−0.987)
pyridoxal (CSF)	MA	5	IVW	0.005	1.231(1.063−1.425)
3−hydroxyhexanoate (Brain)	MA	20	IVW	0.038	1.203(1.010−1.433)
glycosyl ceramide (d18:1/23:1, d17:1/24:1) (Brain)	MA	10	IVW	0.038	1.101(1.005−1.207)
1−oleoyl−GPC (18:1) ((CSF))	MO	17	IVW	0.011	0.587(0.388−0.887)
lysine (CSF)	MO	14	IVW	0.014	0.356(0.157−0.808)
N−acetylglycine (CSF)	MO	13	IVW	0.030	1.579(1.046−2.382)
X−15674 (CSF)	MO	13	IVW	0.040	1.267(1.011−1.589)
2−piperidinone (CSF)	MO	18	IVW	0.041	1.123(1.005−1.255)

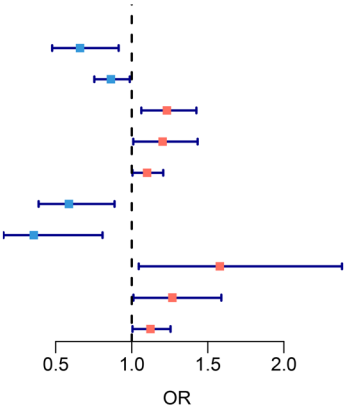

C

Exposure	Outcome (BIPs)	Tissue/Region	nSNP	Method	p−value	OR
Migraine	ISOVF in the right uncinate fasciculus	Association fibers	12	IVW	0.003	1.141(1.047−1.242)
Migraine	MO in the right superior thalamic radiation	Projection fibers	12	IVW	0.024	0.907(0.833−0.987)
Migraine	Cortical surface area of the left postcentral gyrus	Parietal lobe	12	IVW	0.030	0.911(0.837−0.991)
Migraine	MD in the middle cerebellar peduncle	Brainstem tracts	12	IVW	0.045	0.916(0.841−0.998)
MA	Thickness of the left postcentral gyrus	Parietal lobe	35	IVW	0.043	1.042(1.001−1.083)
MO	Cortical surface area of the right rostral middle cingulate cortex	Limbic system	31	IVW	0.003	0.952(0.921−0.983)
MO	Volume of the right rostral middle cingulate cortex	Limbic system	31	IVW	0.010	0.958(0.927−0.990)
MO	ISOVF in the genu of corpus callosum	Commissural fibers	31	IVW	0.042	1.035(1.001−1.069)

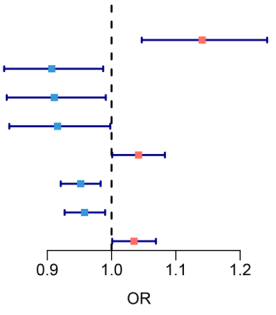

D

Exposure	Outcome (Metabolites)	nSNP	Method	p−value	OR
Migraine	methylmalonate (Brain)	15	IVW	0.026	1.114(1.013−1.226)
Migraine	ascorbic acid 3−sulfate (CSF)	15	IVW	0.027	1.123(1.013−1.244)
Migraine	alpha−hydroxyisovalerate (Brain)	15	IVW	0.046	1.141(1.002−1.299)
MA	N−acetyltaurine (Brain)	39	IVW	0.031	1.042(1.004−1.082)
MO	salicylate (CSF)	4	IVW	0.031	1.364(1.029−1.808)

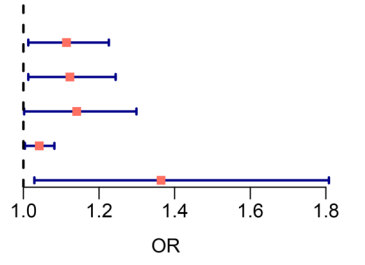

Fig. 3 Bidirectional Mendelian randomization analysis of causal relationships between BIPs, metabolites, and migraine subtypes. (**A**) Forest plot showing the causal effects of BIPs on overall migraine, MA, and MO identified through forward MR analysis. (**B**) Forest plot illustrating the causal effects of CSF and brain metabolites on migraine phenotypes based on forward MR analysis. (**C**) Forest plot of reverse MR results showing the causal effects of migraine and its subtypes on BIPs. (**D**) Forest plot of reverse MR results displaying the causal effects of migraine and its subtypes on CSF and brain metabolites

Table 1 Mediation proportion of metabolites or BIPs in the causal pathways linking BIPs or metabolites to migraine and its subtypes

Exposure	Mediator	Outcome	The Effect of Exposure on Outcome β 1(95% CI)	The Effect of Mediator on Outcome β2 (95% CI)	The Effect of Exposure on Mediator β3 (95% CI)	Mediation effect	Mediated Proportion (%)
Thickness of the right superior parietal gyrus	Nucleotide(CSF)	Overall migraine	−0.274 (−0.407 -−0.141)	−0.148 (−0.282 -−0.013)	0.099 (0.015–0.183)	-0.015	5.328%
Nucleotide(CSF)	Thickness of the left superior parietal gyrus	Overall migraine	−0.148 (−0.282 -−0.013)	−0.206 (−0.338 -−0.075)	0.141 (0.020–0.262)	-0.029	19.691%
Volume of the left lateral occipital cortex	pyridoxal(CSF)	MA	0.201 (0.010–0.393)	−0.559 (−1.037 -−0.080)	−0.041 (−0.080 -−0.002)	0.023	11.444%
ISOVF in the right uncinate fasciculus	X-15,674	MO	0.223 (0.037–0.408)	0.237 (0.011–0.463)	0.097 (0.007–0.187)	0.023	10.292%
lysine(CSF)	Cortical surface area of the left postcentral gyrus	MO	−1.033 (−1.853 -−0.213)	0.216 (0.046–0.386)	−0.524 (−1.005 -−0.043)	-0.113	10.960%

In the case of MA, pyridoxal in CSF served as a mediator in the causal relationship between the volume of the left lateral occipital cortex and MA, accounting for 11.44% of the effect. For MO, two significant mediation pathways were identified: X-15,674 mediated the effect of ISOVF in the right uncinate fasciculus on MO with a 10.29% mediation proportion, and lysine in CSF mediated the effect of cortical surface area in the left postcentral gyrus on MO, explaining 10.96% of the total effect. These findings highlight the presence of cross-omics mediation effects, revealing the intertwined influence of structural brain changes and metabolic alterations in the pathogenesis of migraine. Further details of the mediation analysis analysis can be found in Supplementary Tables 17–19.

The causal effect of gene expression of different brain regions on migraine

Previous two-sample MR analyses identified BIPs with causal associations with migraine, localized to distinct brain regions. Based on this observation, we hypothesized that different brain regions may exert region-specific effects on migraine risk. To investigate this, we conducted a comprehensive SMR analysis using cis-eQTL data from 13 brain region databases to evaluate the causal relationships between gene expression in 13 brain regions and overall migraine as well as its subtypes. This analysis identified 28 genes expressed in the Cerebellar Hemisphere that exhibited causal effects on migraine and its two subtype-related traits. Among these, 14 genes (LY6G5C, RP11-495P10.6, CYP21A2, CD6, INTS1, BTN2A2, SPAG1, ASB16-AS1, CCHCR1, EPHA5, PCDHA3, APTX, PITPNM2, MRPL43) were associated with an increased risk of migraine and its subtypes, including MA and MO (Fig. 5A). Conversely, 14 genes (TOM1L2, SOX7, ALG1L13P, ENPP7P1, RBMS2, FAM86B3P, TMEM132E, ZMYND12, CIB2, RP11-271K11.5, FAM85B, C20orf96, HLA-DQA2, PIGP) were found to be protective, decreasing the risk of migraine and its subtypes (Fig. 5G-I). Our enrichment analysis revealed a strong immunological relevance in the identified pathways. In GO enrichment analysis, the majority of enriched pathways were associated with immune processes, including the positive regulation of T cell activation, leukocyte cell-cell adhesion, lymphocyte activation, and leukocyte activation, as well as pathways related to the MHC class II protein complex and immunological synapse formation (Fig. 5B). Similarly, KEGG enrichment analysis highlighted multiple immune-related pathways, such as antigen processing and presentation, Th1 and Th2 cell differentiation, and Th17 cell differentiation (Fig. 5C). Furthermore, both GO and KEGG analyses identified significant enrichment in pathways related to cell adhesion, including cell adhesion molecules and the positive regulation of cell-cell adhesion. Moreover, we constructed PPI networks (Fig. 5D) and identified potential transcription factors (Fig. 5E) and interacting microRNAs (Fig. 5F) associated with these 28 genes. The Forest plots depicting the causal associations between genes and overall migraine (Fig. 5G), MA (Fig. 5H), and MO (Fig. 5I).

In the amygdala region, we identified 7 genes associated with migraine and its two subtypes, including 3 genes with protective effects and 4 genes linked to an increased risk (Fig S1).

In the anterior cingulate cortex region, we identified 11 genes associated with migraine and its two subtypes, including 6 genes with protective effects and 5 genes linked to an increased risk (Fig S2).

In the Caudate basal ganglia region, we identified 19 genes associated with migraine and its two subtypes,

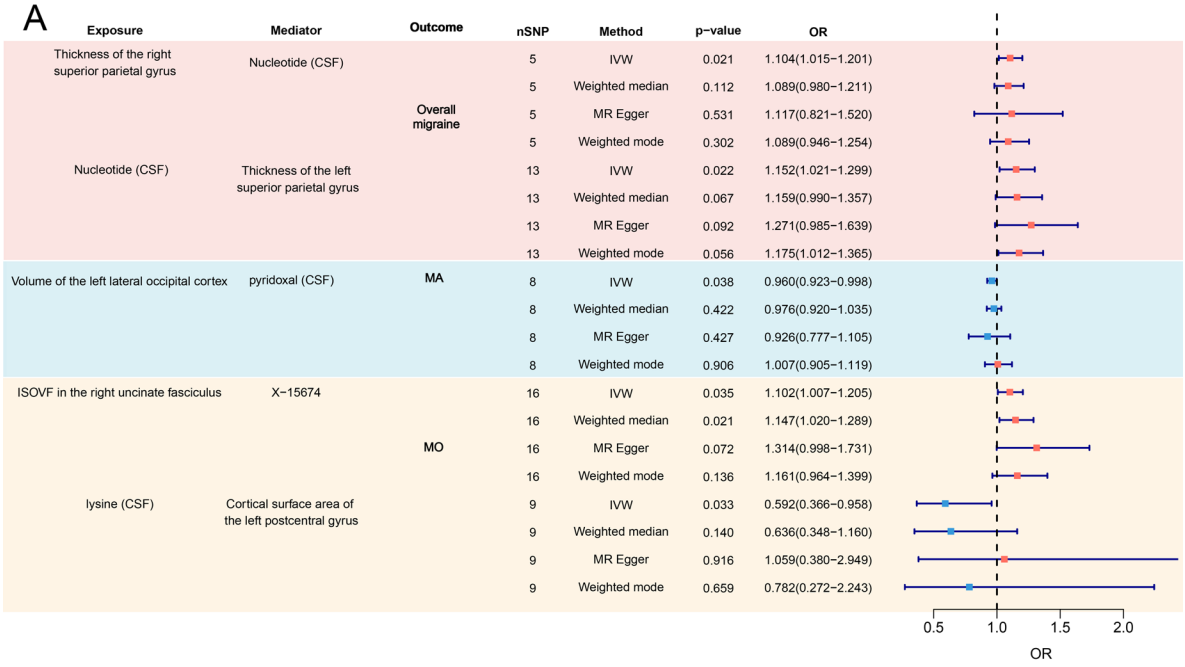

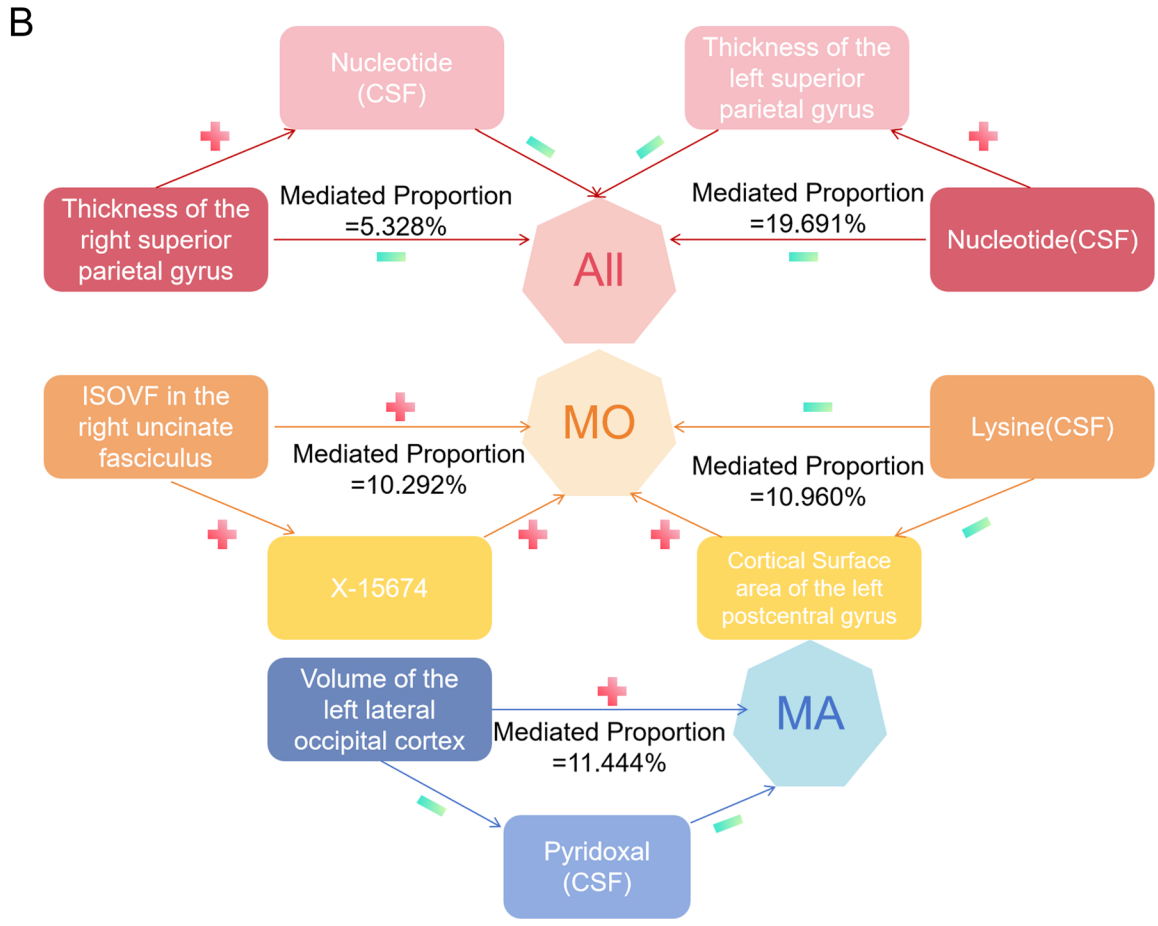

Fig. 4 Mediation analysis reveals cross-omics causal pathways linking brain imaging phenotypes, metabolites, and migraine. (**A**) Forest plot from the second step of two-step MR, assessing causal links between BIPs and metabolites that both demonstrated causal associations with migraine in the first step. (**B**) Schematic summary of five significant mediation pathways identified from two-step MR

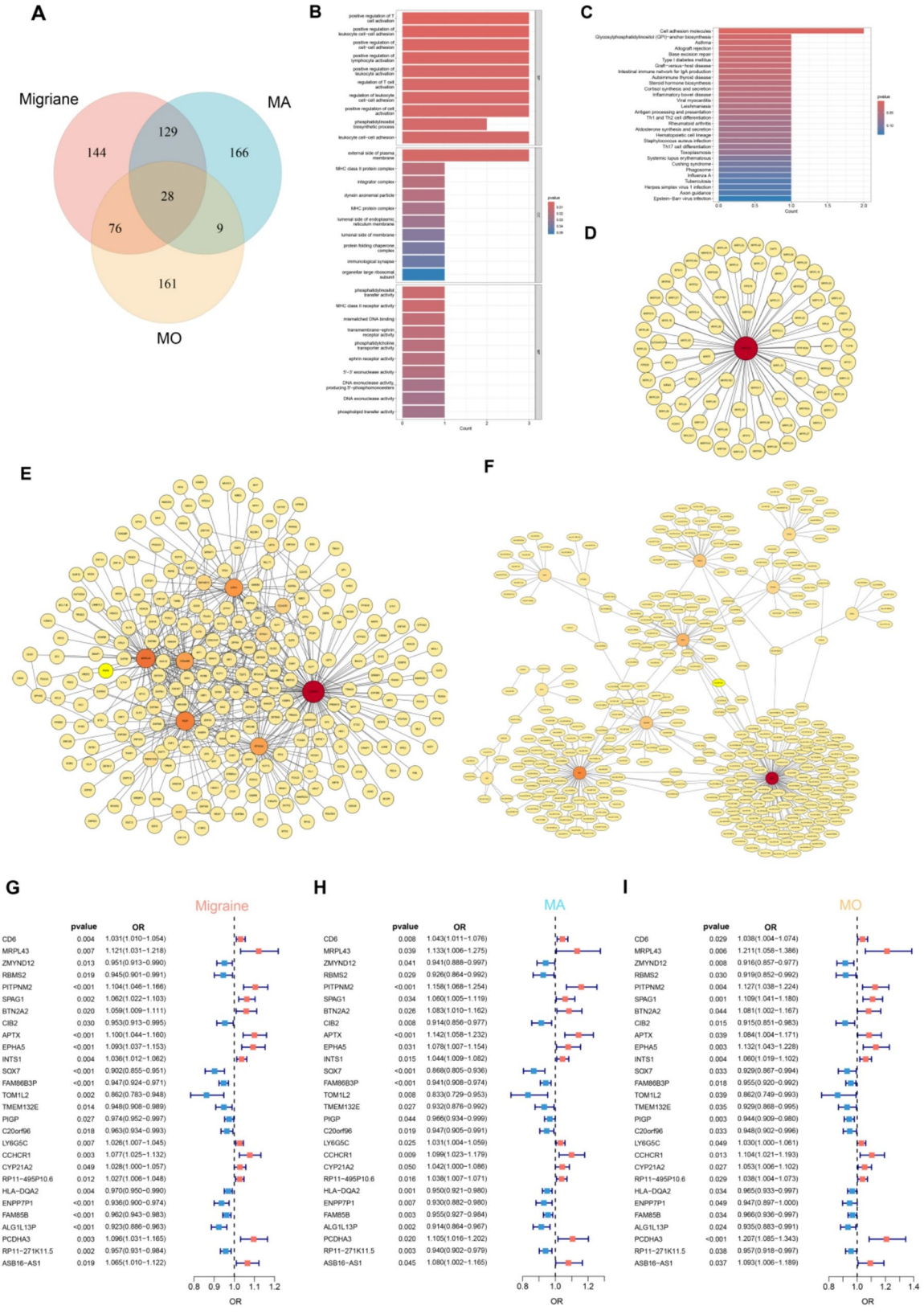

Fig. 5 (See legend on next page.)

(See figure on previous page.)

Fig. 5 The causal effect of gene expression in Cerebellar Hemisphere region on migraine. Venn diagram illustrating gene expression in the brain cerebellar hemisphere with significant causal effects on Migraine, MA, and MO. Numbers indicate unique and shared metabolites among the groups (**A**). GO (**B**) and KEGG (**C**) pathways enriched by genes expressed in the brain cerebellar hemisphere region, exhibiting significant causal effects on Migraine, as well as MA and MO subtypes; the PPI network of screened genes showing the significant causal impact on Migraine, as well as MA and MO subtypes (**D**). The potential translational factors interacted with screened genes, significantly affecting migraine and MA and MO subtypes (**E**). The potential miRNA interacted with screened genes, significantly affecting migraine and MA and MO subtypes (**F**). Forest plot depicting the causal associations between genes and overall migraine (**G**), MA (**H**), and MO (**I**)

including 5 genes with protective effects and 14 genes linked to an increased risk (Fig S3).

In the Cerebellum region, we identified 36 genes associated with migraine and its two subtypes, including 16 genes with protective effects and 20 genes linked to an increased risk (Fig S4).

In the Cortex region, we identified 18 genes associated with migraine and its two subtypes, including 7 genes with protective effects and 11 genes linked to an increased risk (Fig S5).

In the Frontal Cortex region, we identified 23 genes associated with migraine and its two subtypes, including 9 genes with protective effects and 14 genes linked to an increased risk (Fig S6).

In the Hippocampus region, we identified 12 genes associated with migraine and its two subtypes, including 5 genes with protective effects and 7 genes linked to an increased risk (Fig S7).

In the Hypothalamus region, we identified 11 genes associated with migraine and its two subtypes, including 4 genes with protective effects and 7 genes linked to an increased risk (Fig S8).

In the Nucleus accumbens basal ganglia region, we identified 20 genes associated with migraine and its two subtypes, including 7 genes with protective effects and 13 genes linked to an increased risk (Fig S9).

In the Putamen basal ganglia region, we identified 13 genes associated with migraine and its two subtypes, including 4 genes with protective effects and 9 genes linked to an increased risk (Fig S10).

In the Spinal cord cervica region, we identified 12 genes associated with migraine and its two subtypes, including 4 genes with protective effects and 8 genes linked to an increased risk (Fig S11).

In the Substantia nigra region, we identified 5 genes associated with migraine and its two subtypes, including 3 genes with protective effects and 2 genes linked to an increased risk (Fig S12).

Several genes have significant causal effects in multiple brain regions on overall migraine and the MA and MO subtypes. Notably, FAM83B showed a significant association across 13 brain regions, while CIB2 was implicated in 11 brain regions, with both displaying an inhibitory effect. These findings suggest that these genes may play a pivotal role in the neurobiological mechanisms underlying migraine susceptibility and its subtypes, potentially influencing multiple functional networks across the brain. The detailed results of the SMR analysis are provided in Supplementary Table 20.

Discussion

To our knowledge, this is the first study to integrate brain imaging, metabolite, and gene expression data to dissect the genetic mechanisms underlying migraine subtypes. We first used LDSC to explore genetic correlations among BIPs, CSF and brain metabolites, and migraine. By performing bidirectional TSMR, we systematically assessed causal relationships and further applied a two-step TSMR framework to identify cross-omics mediation effects. Subsequently, we conducted a SMR analysis across 13 distinct brain regions to evaluate the causal roles of regional gene expression in migraine and its subtypes. These analyses revealed that brain structural alterations influence migraine risk in part through brain and CSF metabolites, while metabolite levels can also modulate brain imaging phenotypes. Furthermore, SMR analysis suggested that genes with a causal effect on migraine may influence migraine susceptibility through immune-related pathways. Our study highlights a complex and interconnected pathophysiology in migraine.

Using LDSC, we identified significant genetic correlations between migraine and brain metabolites and BIPs. The results reveal substantial genetic associations, indicating a complex interplay between neurological structures, metabolic profile, and migraine pathophysiology. Our findings align with existing research, further supporting the complex genetic basis of migraine [45, 46]. We further performed KEGG enrichment analysis on the metabolites that showed significant genetic correlations with migraine. Across overall migraine as well as the MA and MO subtypes, we observed consistent enrichment of multiple amino acid metabolism-related pathways. Notably, pathways such as glycine, serine and threonine metabolism, and valine, leucine and isoleucine biosynthesis and degradation were prominently represented. These findings suggest that disturbances in amino acid homeostasis may play a functional role in migraine pathogenesis. Supporting this, loss-of-function mutations affecting the α2-Na+/K + ATPase have been shown to cause familial hemiplegic migraine (FHM). A recent study by Sarah Smith and colleagues demonstrated that dysfunction of α2-Na+/K + ATPase, specifically in astrocytes, can evoke episodic paralysis in mice, which was associated with elevated levels of serine and glycine in

the brain [47]. In line with these experimental results, clinical metabolomic studies have also identified altered amino acid profiles in migraine patients. Izabela et al. found elevated levels of histidine in migraine patients both with and without aura, whereas decreased levels of valine and leucine were observed specifically in patients with migraine without aura [48]. Our finding collectively underscore the importance of amino acid metabolism in migraine pathogenesis. Future studies are warranted to further delineate how specific metabolic disruptions influence neuronal and glial function, and to evaluate the therapeutic potential of modulating amino acid pathways as a targeted intervention for different migraine subtypes.

Building on our finding that most migraine associated BIPs map to the parietal lobe. The parietal lobe forms a key subdivision of the cerebral cortex and comprises two principal functional areas: the somatosensory cortex, which receives and processes tactile, proprioceptive, and other sensory inputs from the body and environment; and the posterior parietal cortex, which performs concurrent summaries and higher cognitive functions [49]. Cortical spreading depression (CSD) is a wave of neuronal and glial depolarization that propagates across the cerebral cortex and is considered the neurophysiological correlate of migraine aura [50].Recent neuroimaging studies further underscore the parietal lobe's key role in migraine, particularly in patients with aura. CSD events originating in the parietal cortex can trigger sensory disturbances such as tingling and numbness [51]. Importantly, the neuronal and vascular responses to CSD are complex, involving the release of various vasoactive agents [52], thereby altering metabolic levels within the brain and CSF. Given these intricate neurovascular and metabolic interactions, further studies are required to elucidate the precise molecular mechanisms by which CSD modulates parietal lobe function via metabolic changes.

Our mediation analysis provides novel evidence supporting the presence of cross-omics regulatory pathways in migraine pathogenesis. Specifically, we identified five robust mediation effects involving BIPs and CSF metabolites, underscoring the dynamic interplay between brain structural features and metabolic alterations in shaping migraine risk. In overall migraine, the protective effect of right superior parietal gyrus thickness was partially mediated by CSF nucleotide levels, while the effect of nucleotides on migraine was partially mediated by the thickness of the left superior parietal gyrus. These bidirectional mediation suggests a potential feedback regulatory mechanism between structural alterations in the parietal cortex and purine metabolism, collectively influencing migraine pathogenesis. Purine metabolites such as ATP, ADP, AMP, and adenosine play dual roles in migraine pathophysiology by modulating both vascular tone and nociceptive signaling through P2X and P2Y receptors. Dysregulated purinergic signaling contributes to neurogenic inflammation, cortical spreading depression, and trigeminovascular system activation, which are key mechanisms in migraine onset and progression [53]. It is conceivable that nucleotides and the parietal cortex interact to form a neuroprotective circuit that mitigates migraine susceptibility. Extracellular nucleotides such as ATP can act through purinergic receptors in the parietal cortex to regulate neuronal excitability and modulate pain-related sensory processing. Conversely, the structural integrity of the parietal cortex may help maintain balanced nucleotide metabolism by modulating neuronal activity and glial function. This bidirectional relationship could establish a homeostatic feedback loop that suppresses migraine initiation by simultaneously regulating brain metabolism and cortical excitability.

Previous two-sample MR analyses identified BIPs with causal associations with migraine, localized to distinct brain regions. Based on this observation, we hypothesized that different brain regions may exert region-specific effects on migraine risk. To investigate this, we conducted a comprehensive SMR to evaluate the causal relationships between gene expression in 13 brain regions and migraine. In addition, we performed enrichment analyses, PPI network construction, and TF and miRNA regulatory analyses to further explore the potential underlying mechanisms. Our enrichment analysis revealed significant enrichment of these genes in immune-related pathways. GO enrichment analysis revealed significant enrichment in pathways related to T cell activation, lymphocyte activation, and leukocyte activation, highlighting the potential involvement of immune cell interactions and inflammatory processes in the pathophysiology of migraine. Furthermore, these genes were strongly associated with the MHC class II protein complex and the immune synapse formation pathway. This suggests that antigen presentation and immune signalling may be core migraine susceptibility mechanisms. Similarly, KEGG pathway enrichment analysis identified multiple immune-related signalling pathways, including antigen processing and presentation, Th1 and Th2 cell differentiation, and Th17 cell differentiation. Given their essential role in shaping immune responses, these findings suggest that distinct subpopulations of helper T cells may contribute to the onset and progression of migraine through the modulation of neuroinflammatory pathways. Emerging evidence suggests a strong link between migraine pathophysiology, inflammation, and immune cell activity. The activation of immune pathways may influence the trigeminovascular system [54, 55], and elevated levels of inflammatory cytokines, including IL-6, TNF-α and calcitonin gene-related peptide (CGRP), play

a role in pain transmission and vascular changes during migraine attacks [54, 56, 57].

Notably, FAM83B exhibited significant associations in all 13 brain regions analyzed. Although its role in neural or immune function remains underexplored, FAM83B has been shown to impede the translocation of calbindin 2 (CALB2) from the cytoplasm to the mitochondria, thereby inhibiting apoptosis and enhancing mitochondrial activity [58]. It is plausible that FAM83B may exert a neuroprotective effect in migraine. By promoting mitochondrial function and reducing neuronal vulnerability to metabolic stress, FAM83B may help stabilize neuronal excitability thresholds and reduce susceptibility to migraine attacks. This mechanistic hypothesis aligns with our findings of a consistent inhibitory effect of FAM83B across multiple brain regions.

These findings emphasize that brain structure and metabolic processes are not acting in isolation but are mechanistically interconnected. Our MR analysis revealed distinct genetic characteristics among total migraine, MA, and MO. These findings underscore the divergent neurobiological mechanisms underlying MA and MO, suggesting that they may have distinct genetic and pathophysiological underpinnings despite their shared symptomatic features. These results further indicate that tailored therapeutic strategies, accounting for each subtype's specific genetic and neurobiological profiles, may be essential for optimizing treatment efficacy.

This study employed a large sample size and instrumental factors obtained from the GWAS database, which enhanced the statistical power to predict causal associations and increased the reliability of the results. However, it is imperative to consider our study's particular constraints. The genetic instruments and sample size still limit causal inference. The selected genetic variants may not fully capture the complex genetic background of these diseases. In addition, the findings of this study are derived from data collected from the European population, indicating that there could be substantial limitations on the applicability of its results.

Despite these limitations, our findings provide valuable insights into the potential causal relationships among brain region-specific gene expression, BIPs, brain and CSF metabolites, and migraine, thereby highlighting potential therapeutic targets.

Supplementary Information

The online version contains supplementary material available at https://doi.org/10.1186/s10194-025-02063-7.

Supplementary Material 1

Supplementary Material 2

Supplementary Material 3

Acknowledgements
We thank the participants and investigators of the FinnGen study and the GWAS Resource for public data. I would like to acknowledge my teammates for their wonderful collaboration.

Author contributions
PAZ: Software, Data curation, Writing– original draft. JLW: Conceptualization, Writing– original draft, Investigation. MHD: Investigation, Data curation. XCH: Formal analysis. NJL: Formal analysis, Investigation, Writing– review & editing. RDQ: Formal analysis, Investigation, Writing– review & editing. JL: Supervision, Formal analysis, Writing– review & editing, Funding acquisition. All authors read and approved the final manuscript.

Funding
This work was supported by the National Natural Science Foundation of China (82161138020, 82300040, U1801286), the Science and Technology Program of Guangzhou (202102010011); the Zhongnanshan Medical Foundation of Guangdong Province (ZNSA-2020003, ZNSA-2020013).

Data availability
All data needed to evaluate the conclusions are presented in the paper. The resources, tools, and codes used in our analyses were described in the methods section.

Declarations

Ethical approval
The data for this investigation were acquired from previously published studies and public sources, negating the need for further ethical approval.

Competing interests
The authors declare no competing interests.

Author details
[1]Department of Allergy and Clinical Immunology, State Key Laboratory of Respiratory Disease, National Clinical Research Center for Respiratory Disease, Guangzhou Institute of Respiratory Health, The First Affiliated Hospital of Guangzhou Medical University, No.151, Yanjiangxi Road, Yuexiu District, Guangzhou, Guangdong 510120, China
[2]Department of Obstetrics and Gynecology, Department of Gynecologic Oncology Research Office, Guangzhou Key Laboratory of Targeted Therapy for Gynecologic Oncology, Guangdong Provincial Key Laboratory of Major Obstetric Diseases, Guangdong Provincial Clinical Research Center for Obstetrics and Gynecology, Guangdong-Hong Kong-Macao Greater Bay Area Higher Education Joint Laboratory of Maternal-Fetal Medicine, The Third Affiliated Hospital, Guangzhou Medical University, Guangzhou, China

Received: 11 March 2025 / Accepted: 3 May 2025
Published online: 20 May 2025

References

1. Headache Classification Committee of the International Headache Society (IHS) The International Classification of Headache Disorders, 3rd edition. Cephalalgia (2018) 38:1-211
2. Steiner TJ, Stovner LJ (2023) Global epidemiology of migraine and its implications for public health and health policy. Nat Rev Neurol 19:109–117
3. Dodick DW (2018) Migraine Lancet 391:1315–1330
4. Ashina S, Bentivegna E, Martelletti P, Eikermann-Haerter K (2021) Structural and functional brain changes in migraine. Pain Ther 10:211–223
5. Lai KL, Niddam DM (2020) Brain metabolism and structure in chronic migraine. Curr Pain Headache Rep 24:69
6. Barbiroli B, Montagna P, Cortelli P, Funicello R, Iotti S, Monari L, Pierangeli G, Zaniol P, Lugaresi E (1992) Abnormal brain and muscle energy metabolism shown by 31P magnetic resonance spectroscopy in patients affected by migraine with aura. Neurology 42:1209–1214
7. Bell T, Stokoe M, Khaira A, Webb M, Noel M, Amoozegar F, Harris AD (2021) GABA and glutamate in pediatric migraine. Pain 162:300–308

8. Zhang X, Wang W, Bai X, Zhang Y, Yuan Z, Tang H, Zhang X, Li Z, Zhang P, Hu Z et al (2023) Changes in gamma-aminobutyric acid and glutamate/glutamine levels in the right thalamus of patients with episodic and chronic migraine: A proton magnetic resonance spectroscopy study. Headache 63:104–113
9. Zunhammer M, Schweizer LM, Witte V, Harris RE, Bingel U, Schmidt-Wilcke T (2016) Combined glutamate and glutamine levels in pain-processing brain regions are associated with individual pain sensitivity. Pain 157:2248–2256
10. Vollono C, Primiano G, Della MG, Losurdo A, Servidei S (2018) Migraine in mitochondrial disorders: prevalence and characteristics. Cephalalgia 38:1093–1106
11. Wang Y, Wang Y, Yue G, Zhao Y (2023) Energy metabolism disturbance in migraine: from a mitochondrial point of view. Front Physiol 14:1133528
12. Eikermann-Haerter K, Arbel-Ornath M, Yalcin N, Yu ES, Kuchibhotla KV, Yuzawa I, Hudry E, Willard CR, Climov M, Keles F et al (2015) Abnormal synaptic Ca(2+) homeostasis and morphology in cortical neurons of Familial hemiplegic migraine type 1 mutant mice. Ann Neurol 78:193–210
13. Theriot JJ, Toga AW, Prakash N, Ju YS, Brennan KC (2012) Cortical sensory plasticity in a model of migraine with aura. J Neurosci 32:15252–15261
14. Wen P, Sun Z, Gou F, Wang J, Fan Q, Zhao D, Yang L (2025) Oxidative stress and mitochondrial impairment: key drivers in neurodegenerative disorders. Ageing Res Rev 104:102667
15. Yu Y, Herman P, Rothman DL, Agarwal D, Hyder F (2018) Evaluating the Gray and white matter energy budgets of human brain function. J Cereb Blood Flow Metab 38:1339–1353
16. Emdin CA, Khera AV, Kathiresan S (2017) Mendelian randomization. JAMA 318:1925
17. Sekula P, Del GMF, Pattaro C, Köttgen A (2016) Mendelian randomization as an approach to assess causality using observational data. J Am Soc Nephrol 27:3253–3265
18. Hemani G, Zheng J, Elsworth B, Wade KH, Haberland V, Baird D, Laurin C, Burgess S, Bowden J, Langdon R et al (2018) The MR-Base platform supports systematic causal inference across the human phenome. Elife 7
19. Smith GD, Lawlor DA, Harbord R, Timpson N, Day I, Ebrahim S (2007) Clustered environments and randomized genes: a fundamental distinction between conventional and genetic epidemiology. Plos Med 4:e352
20. Wootton RE, Richmond RC, Stuijfzand BG, Lawn RB, Sallis HM, Taylor G, Hemani G, Jones HJ, Zammit S, Davey SG, Munafò MR (2020) Evidence for causal effects of lifetime smoking on risk for depression and schizophrenia: a Mendelian randomisation study. Psychol Med 50:2435–2443
21. Tanha HM, Sathyanarayanan A, Nyholt DR (2021) Genetic overlap and causality between blood metabolites and migraine. Am J Hum Genet 108:2086–2098
22. Mitchell BL, Diaz-Torres S, Bivol S, Cuellar-Partida G, Gerring ZF, Martin NG, Medland SE, Grasby KL, Nyholt DR, Rentería ME (2022) Elucidating the relationship between migraine risk and brain structure using genetic data. Brain 145:3214–3224
23. Sun Z, Liu M, Zhao G, Zhang Z, Xu J, Song L, Zhang W, Wang S, Jia L, Wu Q et al (2024) Causal relationships between cortical brain structural alterations and migraine subtypes: a bidirectional Mendelian randomization study of 2,347 neuroimaging phenotypes. J Headache Pain 25:186
24. Pang Z, Lu Y, Zhou G, Hui F, Xu L, Viau C, Spigelman AF, MacDonald PE, Wishart DS, Li S, Xia J (2024) MetaboAnalyst 6.0: towards a unified platform for metabolomics data processing, analysis and interpretation. Nucleic Acids Res 52:W398–W406
25. Emdin CA, Khera AV, Kathiresan S (2017) Mendelian randomization. JAMA 318:1925–1926
26. Skrivankova VW, Richmond RC, Woolf B, Yarmolinsky J, Davies NM, Swanson SA, VanderWeele TJ, Higgins J, Timpson NJ, Dimou N et al (2021) Strengthening the reporting of observational studies in epidemiology using Mendelian randomization: the STROBE-MR statement. JAMA 326:1614–1621
27. Smith SM, Douaud G, Chen W, Hanayik T, Alfaro-Almagro F, Sharp K, Elliott LT (2021) An expanded set of genome-wide association studies of brain imaging phenotypes in UK biobank. Nat Neurosci 24:737–745
28. Guo J, Yu K, Dong SS, Yao S, Rong Y, Wu H, Zhang K, Jiang F, Chen YX, Guo Y, Yang TL (2022) Mendelian randomization analyses support causal relationships between brain imaging-derived phenotypes and risk of psychiatric disorders. Nat Neurosci 25:1519–1527
29. Wang C, Yang C, Western D, Ali M, Wang Y, Phuah CL, Budde J, Wang L, Gorijala P, Timsina J et al (2024) Genetic architecture of cerebrospinal fluid and brain metabolite levels and the genetic colocalization of metabolites with human traits. Nat Genet 56:2685–2695
30. Kurki MI, Karjalainen J, Palta P, Sipilä TP, Kristiansson K, Donner KM, Reeve MP, Laivuori H, Aavikko M, Kaunisto MA et al (2023) FinnGen provides genetic insights from a well-phenotyped isolated population. Nature 613:508–518
31. Verbanck M, Chen CY, Neale B, Do R (2018) Detection of widespread horizontal Pleiotropy in causal relationships inferred from Mendelian randomization between complex traits and diseases. Nat Genet 50:693–698
32. You D, Wu Y, Lu M, Shao F, Tang Y, Liu S, Liu L, Zhou Z, Zhang R, Shen S et al (2025) A genome-wide cross-trait analysis characterizes the shared genetic architecture between lung and Gastrointestinal diseases. Nat Commun 16:3032
33. Zhang B, He W, Pei Z, Guo Q, Wang J, Sun M, Yang X, Ariben J, Li S, Feng W et al (2024) Plasma proteins, Circulating metabolites mediate causal inference studies on the effect of gut bacteria on the risk of osteoporosis development. Ageing Res Rev 101:102479
34. Zheng J, Erzurumluoglu AM, Elsworth BL, Kemp JP, Howe L, Haycock PC, Hemani G, Tansey K, Laurin C, Pourcain BS et al (2017) LD hub: a centralized database and web interface to perform LD score regression that maximizes the potential of summary level GWAS data for SNP heritability and genetic correlation analysis. Bioinformatics 33:272–279
35. Bulik-Sullivan BK, Loh PR, Finucane HK, Ripke S, Yang J, Patterson N, Daly MJ, Price AL, Neale BM (2015) LD score regression distinguishes confounding from polygenicity in genome-wide association studies. Nat Genet 47:291–295
36. Bowden J, Del GMF, Minelli C, Davey SG, Sheehan N, Thompson J (2017) A framework for the investigation of Pleiotropy in two-sample summary data Mendelian randomization. Stat Med 36:1783–1802
37. Pan H, Liu CX, Zhu HJ, Zhang GF (2024) Immune cells mediate the effects of gut microbiota on neuropathic pain: a Mendelian randomization study. J Headache Pain 25:196
38. Cui ZY, Feng H, He BC, He JY, Tian H, Tian Y (2023) Causal associations between serum amino acid levels and osteoarthritis: a Mendelian randomization study. Osteoarthritis Cartilage 31:1121–1131
39. Cohen JF, Chalumeau M, Cohen R, Korevaar DA, Khoshnood B, Bossuyt PM (2015) Cochran's Q test was useful to assess heterogeneity in likelihood ratios in studies of diagnostic accuracy. J Clin Epidemiol 68:299–306
40. Bowden J, Davey SG, Burgess S (2015) Mendelian randomization with invalid instruments: effect Estimation and bias detection through Egger regression. Int J Epidemiol 44:512–525
41. Bowden J, Davey SG, Haycock PC, Burgess S (2016) Consistent Estimation in Mendelian randomization with some invalid instruments using a weighted median estimator. Genet Epidemiol 40:304–314
42. Liu Z, Wang H, Yang Z, Lu Y, Zou C (2023) Causal associations between type 1 diabetes mellitus and cardiovascular diseases: a Mendelian randomization study. Cardiovasc Diabetol 22:236
43. Sanderson E (2021) Multivariable Mendelian randomization and mediation. Cold Spring Harb Perspect Med 11
44. Zhou G, Soufan O, Ewald J, Hancock R, Basu N, Xia J (2019) NetworkAnalyst 3.0: a visual analytics platform for comprehensive gene expression profiling and meta-analysis. Nucleic Acids Res 47:W234–W241
45. Grech O, Sassani M, Terwindt G, Lavery GG, Mollan SP, Sinclair AJ (2022) Alterations in metabolic flux in migraine and the translational relevance. J Headache Pain 23:127
46. Acarsoy C, Ikram MK, Ikram MA, Vernooij MW, Bos D (2024) Migraine and brain structure in the elderly: the Rotterdam study. Cephalalgia 44:2069655289
47. Smith SE, Chen X, Brier LM, Bumstead JR, Rensing NR, Ringel AE, Shin H, Oldenborg A, Crowley JR, Bice AR et al (2020) Astrocyte deletion of α2-Na/K ATPase triggers episodic motor paralysis in mice via a metabolic pathway. Nat Commun 11:6164
48. Domitrz I, Koter MD, Cholojczyk M, Domitrz W, Baranczyk-Kuzma A, Kaminska A (2015) Changes in serum amino acids in migraine patients without and with aura and their possible usefulness in the study of migraine pathogenesis. CNS Neurol Disord Drug Targets 14:345–349
49. Souza-Couto D, Bretas R, Aversi-Ferreira TA (2023) Neuropsychology of the parietal lobe: Luria's and contemporary conceptions. Front Neurosci 17:1226226
50. Costa C, Tozzi A, Rainero I, Cupini LM, Calabresi P, Ayata C, Sarchielli P (2013) Cortical spreading depression as a target for anti-migraine agents. J Headache Pain 14:62
51. Gollion C, Christensen RH, Ashina H, Al-Khazali HM, Fisher PM, Amin FM, Lauritzen M, Ashina M (2025) Somatosensory migraine auras evoked by

bihemispheric cortical spreading depression events in human parietal cortex. J Cereb Blood Flow Metab 45:558–567
52. Ayata C, Lauritzen M (2015) Spreading depression, spreading depolarizations, and the cerebral vasculature. Physiol Rev 95:953–993
53. Biringer RG (2023) Migraine signaling pathways: purine metabolites that regulate migraine and predispose migraineurs to headache. Mol Cell Biochem 478:2813–2848
54. Messlinger K (2018) The big CGRP flood - sources, sinks and signalling sites in the trigeminovascular system. J Headache Pain 19:22
55. Lin J, Zhou L, Luo Z, Adam MI, Zhao L, Wang F, Luo D (2021) Flow cytometry analysis of immune and glial cells in a trigeminal neuralgia rat model. Sci Rep 11:23569
56. Yücel M, Kotan D, Gurol ÇG, Çiftçi IH, Cikriklar HI (2016) Serum levels of endocan, claudin-5 and cytokines in migraine. Eur Rev Med Pharmacol Sci 20:930–936
57. Bruno PP, Carpino F, Carpino G, Zicari A (2007) An overview on immune system and migraine. Eur Rev Med Pharmacol Sci 11:245–248
58. Wang J, Li P, Sun L, Zhang J, Yue K, Wang Y, Wu X (2024) FAM83B regulates mitochondrial metabolism and anti-apoptotic activity in pulmonary adenocarcinoma. Apoptosis 29:743–756

Publisher's note